Journal of Digital Imaging (2019) 32:241–250
https://doi.org/10.1007/s10278-019-00178-3

Anthropometer3D: Automatic Multi-Slice Segmentation Software for the Measurement of Anthropometric Parameters from CT of PET/CT

Pierre Decazes [1,2] · David Tonnelet [1] · Pierre Vera [1,2] · Isabelle Gardin [1,2]

Published online: 12 February 2019

Abstract

Anthropometric parameters like muscle body mass (MBM), fat body mass (FBM), lean body mass (LBM), visceral adipose tissue (VAT), and subcutaneous adipose tissue (SAT) are used in oncology. Our aim was to develop and evaluate the software Anthropometer3D measuring these anthropometric parameters on the CT of PET/CT. This software performs a multi-atlas segmentation of CT of PET/CT with extrapolation coefficients for the body parts beyond the usual acquisition range (from the ischia to the eyes). The multi-atlas database is composed of 30 truncated CTs manually segmented to isolate three types of voxels (muscle, fat, and visceral fat). To evaluate Anthropomer3D, a leave-one-out cross-validation was performed to measure MBM, FBM, LBM, VAT, and SAT. The reference standard was based on the manual segmentation of the corresponding whole-body CT. A manual segmentation of one CT slice at level L3 was also used. Correlations were analyzed using Dice coefficient, intra-class coefficient correlation (ICC), and Bland–Altman plot. The population was heterogeneous (sex ratio 1:1; mean age 57 years old [min 23; max 74]; mean BMI 27 kg/m^2 [min 18; max 40]). Dice coefficients between reference standard and Anthropometer3D were excellent (mean+/-SD): muscle 0.95 ± 0.02, fat 1.00 ± 0.01, and visceral fat 0.97 ± 0.02. The ICC was almost perfect (minimal value of 95% CI of 0.97). All Bland–Altman plot values (mean difference, 95% CI and slopes) were better for Anthropometer3D compared to L3 level segmentation. Anthropometer3D allows multiple anthropometric measurements based on an automatic multi-slice segmentation. It is more precise than estimates using L3 level segmentation.

Keywords Body composition · Positron emission tomography · Computed tomography · Multi-atlas segmentation

Background

Body composition extracted from medical images is increasingly important in oncology. The total skeletal muscle body mass (MBM) measurement is used to determine muscle depletion, which is a significant prognostic factor in cancer [1]. It has been associated with a higher incidence of chemotherapy toxicity, a shorter time to tumor progression, poorer surgical outcomes, impaired functional status, and shorter survival, especially in the case of muscle loss during the treatment [2–4]. Obesity, which can be assessed by measuring fat body mass (FBM) [5], is a well-known risk factor for many cancers [6] that can modify tolerance to chemotherapy [7]. Conversely, adipopenia is a negative prognostic factor, notably for hematologic cancer [8]. Low lean body mass (LBM) is a significant predictor of toxicity and neuropathy in patients treated with folinic acid, fluorouracil, and oxaliplatin (FOLFOX)-based regimens. Visceral adipose tissue (VAT) and the ratio of VAT to subcutaneous adipose tissue (SAT) are prognostic and/or predictive factors for many solid tumors [9, 10]. For example, because patients with a large VAT mass may not benefit from bevacizumab-based chemotherapy, measurement of VAT before starting this treatment could be useful [11]. To summarize, these parameters could reflect the patient's health status (notably MBM), but also the distribution volume of the chemotherapy (notably FBM and LBM), both of which are important to determine on how to adapt the treatment and follow-up of the patient.

All these parameters can be accurately measured in three-dimensional (3D) imaging on computed tomography (CT) or magnetic resonance imaging (MRI) [12]. Although CT offers well-defined Hounsfield unit (HU) values and contrast for muscle and fat voxels easily extracted [13], it exposes subjects

✉ Pierre Decazes
pierre.decazes@chb.unicancer.fr

[1] Department of Nuclear Medicine, Henri Becquerel Cancer Center, Rouen, France

[2] LITIS-QuantIF-EA4108, University of Rouen, Rouen, France

to ionizing radiation, and it is unethical to perform a CT for only measuring anthropometric parameters [14]. This limitation is overcome for patients who routinely undergo CT examinations, alone or combined with positron emission tomography (PET), to evaluate and follow the disease [15]. Anthropometric measurement can, therefore, be performed on these images, in particular, by taking advantage of the large acquisition range, at least from the ischium to the eyes for PET/CT, using multi-slice segmentation [16, 17].

It was proposed to estimate MBM, LBM, FBM, VAT, and SAT from a two-dimensional (2D) segmentation of one slice at level L3 [15, 18]. Two-dimensional estimates are based on mathematical expressions assuming a strong correlation between these estimates (2D) and volume quantities (3D). However, 2D estimates could be less accurate than 3D multi-slice measurements [17]. For example, it has been shown that during weight loss, changes in visceral and subcutaneous adipose tissue are poorly evaluated on 2D imaging [19], while 3D imaging gives good results for intra-abdominal fat [20]. Therefore, multi-slice segmentation is preferable [21], but needs automatic processing to avoid a time-consuming manual segmentation [19].

To perform a 3D segmentation of these tissues, few automatic segmentation methods have been proposed [e.g., region growing, graph cutting, fuzzy C means clustering, and multi-atlas segmentation (MAS) algorithms] [22]. Most of them are based on the determination of the muscle boundary between VAT and SAT [22]. Among them, MAS methods are very flexible and can capture anatomical variations, notably between different levels of the body, such as the abdomen or the pelvis [23], whereas other algorithms must be adapted according to the anatomical level [24] and are composed of several methods to cover the whole body. MAS methods have shown accurate measurement capabilities, particularly in MRI [25]. However, to our knowledge, there is no software available to automatically measure all parameters from CT of PET/CT using multi-slice segmentation, although this is an examination commonly done for patients with cancer.

The aim of our study was to develop an in-house software, called Anthropometer3D, allowing the automatic measurements of all these anthropometric parameters from CT of PET/CT with a limited range of acquisition from the ischium to the eyes, and to compare these measurements to those obtained by manual segmentation on a whole-body CT, as a reference, and on a single slice at level L3.

Methods

Population

This is a retrospective, non-interventional study approved by the institutional review board. All patients were informed that their anonymized images could be used for research purposes and that they could object to such use. Thirty random patients (15 women and 15 men) who underwent whole-body PET/CT (GE Discovery 710 with Optima 660 CT component) between June 2016 and July 2017 during follow-up of their disease and with complete tumor response (no tumor visualized) were included.

After a 6-h fast and 30 min of rest, patients were injected with 3.5 MBq/kg of ^{18}F-fluorodeoxyglucose (^{18}F-FDG). Sixty minutes later, a CT scan in the craniocaudal direction was performed with the patient's arms positioned above the head and the patient breathing freely. CT acquisition parameters depended on the patient's body mass index (BMI). For patients with a BMI less than 30 kg/m^2, the CT voltage was 100 kV; otherwise, the CT voltage was 120 kV. The CT mAs was automatically regulated by the manufacturer's dose reduction software based on a noise index. The result was a mean effective mAs of 89.1 ± 6.7. Each CT scan was acquired with primary collimation of 16 × 1.25 mm and reconstructed in 3.75-mm thick slices every 3.27 mm. All images were resized to obtain a unique voxel size of 1.36 × 1.36 × 5 mm^3.

Anthropometer3D

The aim of the Anthropometer3D software is to allow an automatic measurement of multiple anthropometric parameters. This tool could notably be applied on large clinical databases to explore new prognostic factors, in particular within the framework of academic collaborations via the website https://www.anthropometer3d.org [26], where the software will be released online upon acceptance of this paper. Figure 1 provides a graphical representation of the Anthropometer3D software process. Anthropometer3D is a command line software written in Java language which uses ImageJ software functions for parts of image processing and the software Plastimatch for the elastic registration parts. It is based on a MAS method involving the recording of several CT atlases corresponding to training images that have already been labeled into three different masks by an expert. Then, personalized masks are created on the patient's CT scan to be analyzed in order to segment the tissues of interest. The three masks used by Anthropometer3D are as follows: one for the body shape used to calculate $FBM_{Anthopo3D}$ and $LBM_{Anthopo3D}$ (Mask1), one for the abdominal cavity used to calculate $VAT_{Anthopo3D}$ and $SAT_{Anthopo3D}$ (Mask2), and one for the muscles used to calculate $MBM_{Anthopo3D}$ (Mask3).

Considering that the body part from the ischium to the eyes is usually included in the acquisition range of a PET/CT, the CT atlases were truncated to keep only this part. During the segmentation, each truncated CT atlas is rigidly registered to the analyzed CT. The mutual information between the rigidly registered CT and the analyzed CT is calculated [27] and the top ten registered CT atlases are selected. They correspond to a morphotype quite similar to that of the patient analyzed. These

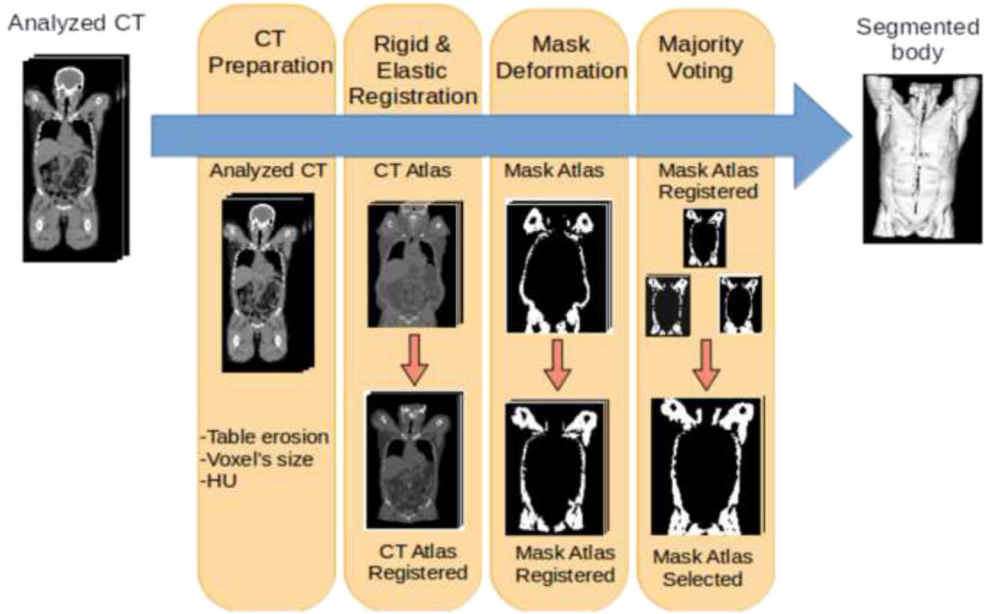

Fig. 1 Graphical representation of the steps of the multi-atlas segmentation method used by Anthropometer3D to segment the muscles

ten selected CT atlas are then elastically registered to the analyzed CT and the resulting deformation fields are applied to the masks. Finally, the three personalized masks are obtained by a majority voting process. To isolate muscle voxels, a threshold is applied to Mask3 (HU values between − 29 and 150 [13]). To isolate fat voxels, a threshold applied on Mask1 and Mask2 (HU values between − 190 and − 30 [13]). As fat and muscle voxels have no HU in common in these windows, no overlap between these tissues was observed. Moreover, subcutaneous fat voxels were obtained by subtracting the visceral fat voxels to the whole-body fat voxels so no overlap was also observed for these segmentations.

Anthropometer3D automatically extrapolates body parts beyond the ischium and eyes to obtain an estimate of whole-body measurements. To account for the underestimation of segmented volumes on the truncated CT relative to the whole-body CT, extrapolation factors, k_{muscle} and k_{fat}, were calculated. They correspond to the average extrapolation factors calculated on the data of the CT atlases as being the ratio between the number of muscle (or fat) voxels determined on the whole-body CT divided by the number of voxels belonging to the muscle (or fat) determined on the truncated CT. The extrapolation factors were calculated by using the CT atlases (whole body and truncated from the eyes to the ischia) manually segmented,

$$\text{With } k_{\text{muscle}} = \frac{\overline{N_{\text{muscle}} \text{of whole-body CT atlas}}}{N_{\text{muscle}} \text{of truncated CT atlas}}$$

And

$$k_{\text{fat}} = \frac{\overline{N_{\text{fat}} \text{of whole-body CT atlas}}}{N_{\text{fat}} \text{of truncated CT atlas}}$$

Then, $\text{MBM}_{\text{Anthopo3D}}$, $\text{FBM}_{\text{Anthopo3D}}$, $\text{LBM}_{\text{Anthopo3D}}$, $\text{VAT}_{\text{Anthopo3D}}$, and $\text{SAT}_{\text{Anthopo3D}}$ are calculated as follows:

$$\text{MBM}_{\text{Anthropo3D}} = N_{\text{muscle}} \times k_{\text{muscle}} \times V_{\text{voxel}} \times \rho_{\text{muscle}}$$
$$\text{FBM}_{\text{Anthropo3D}} = N_{\text{fat}} \times k_{\text{fat}} \times V_{\text{voxel}} \times \rho_{\text{fat}}$$
$$\text{LBM}_{\text{Anthropo3D}} = W - \text{FBM}_{\text{Anthropo3D}}$$
$$\text{VAT}_{\text{Anthropo3D}} = N_{\text{visceral fat}} \times V_{\text{voxel}} \times \rho_{\text{fat}}$$
$$\text{SAT}_{\text{Anthropo3D}} = \text{FBM}_{\text{Anthropo3D}} - \text{VAT}_{\text{Anthropo3D}}$$

With N_{muscle} and N_{fat} being the number of voxels of muscle and fat, respectively, obtained on the truncated CT, W is the patient's weight in g, V_{voxel} is the volume of one voxel (in milliliters), ρ_{muscle} is the density of muscle (equal to 1.06 g/mL) [28], and ρ_{fat} is the density of fat (equal to 0.923 g/mL) [13].

Validation of Anthropometer3D

The segmentation results of Anthropometer3D were compared with two other segmentation methods. The first one is the reference standard corresponding to the measurement of MBM_{REF}, FBM_{REF}, LBM_{REF}, VAT_{REF}, and SAT_{REF} performed on the whole-body CT. Manual segmentation of the muscles, used to determine MBM_{REF}, and of the abdominal cavity, used to determine VAT_{REF} and SAT_{REF}, was performed by two physicians (one junior physician, D.T., with 3 years of experience and one senior physician, P.D., with 7 years of experience) using the software Seg3D 2.4 [29]. A whole-body-shape mask was obtained by an automatic algorithm previously described [17] and was used to calculate FBM_{REF} and LBM_{REF}. To isolate tissue voxels, thresholding was applied with HU values between − 29 and + 150 for muscles and between − 190 and − 30 for fat voxels. All the segmentations

and masks were checked by the senior physician. The reference standard was defined as follows:

$$\mathrm{MBM_{REF}} = N_{\mathrm{muscle}} \times V_{\mathrm{voxel}} \times \rho_{\mathrm{muscle}}$$
$$\mathrm{FBM_{REF}} = N_{\mathrm{fat}} \times V_{\mathrm{voxel}} \times \rho_{\mathrm{fat}}$$
$$\mathrm{LBM_{REF}} = W - \mathrm{FBM_{REF}}$$
$$\mathrm{VAT_{REF}} = N_{\mathrm{visceral\ fat}} \times V_{\mathrm{voxel}} \times \rho_{\mathrm{fat}}$$
$$\mathrm{SAT_{REF}} = \mathrm{FBM_{REF}} - \mathrm{VAT_{REF}}$$

The second segmentation method is based on measurements obtained from manual segmentation of one CT slice at level L3 and the use of mathematical extrapolation formulas given in the literature [15, 18], as follows:

$$\mathrm{MBM_{L3}}$$
$$\text{for women} = \left(0.141 \times \text{Area Muscle}_{\mathrm{L3}}\left(\mathrm{cm}^2\right) + 3.79\right) \times \rho_{\mathrm{muscle}}$$
$$\text{for men} = \left(0.136 \times \text{Area VAT}_{\mathrm{L3}}\left(\mathrm{cm}^2\right) + 5.944\right) \times \rho_{\mathrm{muscle}}$$
$$\mathrm{FBM_{L3}} = 0.042 \times \text{Area Fat}_{\mathrm{L3}}\left(\mathrm{cm}^2\right) + 11.2$$
$$\mathrm{LBM_{L3}} = 0.30 \times \text{Area Muscle}_{\mathrm{L3}}\left(\mathrm{cm}^2\right) + 6.06$$
$$\mathrm{VAT_{L3}}$$
$$\text{for women} = \left(0.026 \times \text{Area VAT}_{\mathrm{L3}}\left(\mathrm{cm}^2\right) + 0.121\right) \times \rho_{\mathrm{fat}}$$
$$\text{for men} = \left(0.025 \times \text{Area VAT}_{\mathrm{L3}}\left(\mathrm{cm}^2\right) + 0.164\right) \times \rho_{\mathrm{fat}}$$
$$\mathrm{SAT_{L3}}$$
$$\text{for women} = \left(0.087 \times \text{Area SAT}_{\mathrm{L3}}\left(\mathrm{cm}^2\right) + 5.92\right) \times \rho_{\mathrm{fat}}$$
$$\text{for men} = \left(0.078 \times \text{Area SAT}_{\mathrm{L3}}\left(\mathrm{cm}^2\right) + 4.487\right) \times \rho_{\mathrm{fat}}$$

To evaluate Anthropometer3D, a leave-one-out cross-validation method was used. $\mathrm{MBM_{Anthopo3D}}$, $\mathrm{FBM_{Anthopo3D}}$, $\mathrm{LBM_{Anthopo3D}}$, $\mathrm{VAT_{Anthopo3D}}$, and $\mathrm{SAT_{Anthopo3D}}$ of each truncated CT of the 30 patients were obtained by using data (CT atlas, masks, and extrapolation factors) of the 29 other CTs in the database.

Statistical Analyses

Descriptive statistics of the population and results were performed with continuous variables reported as mean ± standard deviation (SD), and categorical variables were reported as frequencies (percentages).

The agreement between the five outcomes obtained by Anthropometer3D and the reference standard corresponding to the whole-body manual segmentation was estimated by computing the mean of the intra-class coefficient correlation (ICC) and the corresponding 95% confidence interval (95%CI) [30]. The agreement between two segmentation methods was also studied using Bland–Altman plots [31]. Same statistical analyses were performed for the outcomes obtained by the manual segmentation at level L3. Dice's coefficients between the manually segmented voxels and the automatically segmented voxels in the common range (from ischium to eyes) were also calculated [32].

Statistical analyses were performed using the software R, version 3.4.3 [33].

Results

The characteristics of the 30 patients are provided in Table 1. The 15 women and 15 men had diverse morphotypes, as shown by the mean BMI of 27 kg/m^2, with a minimum value of 18 kg/m^2 and a maximal value of 40 kg/m^2. The descriptive statistics for all measured parameters are provided in Table 2. According to the SD, minimal and maximal values, the distribution was very variable for each parameter, in favor of a heterogeneity of the population.

The result of a patient's segmentation using Antropometer3D is provided in Fig. 2 and the segmentation of six patients (three women and three men) with different body shapes (from a BMI of 20.5 kg/m^2 to a BMI of 39.9 kg/m^2) is presented in Fig. 3.

The whole population's mean extrapolation factor (calculated on the 30 patients with whole-body manually segmented) k_{muscle} was equal to 1.92 (SD ± 0.08, minimal 1.78, maximal 2.06), whereas k_{fat} was equal to 1.44 (SD ± 0.10, minimal 1.30, maximal 1.67).

The Bland–Altman plots between the results of the segmentations obtained with Anthopometer3D and the reference method on the one hand, and with the L3 method and the reference method, on the other hand, are provided in Fig. 4. The results of the Bland–Altman analysis and of ICC and the corresponding 95%CI are presented in Table 3. The ICC between the reference standard and Anthropometer3D were all excellent (minimal value of 95%CI of 0.97), whereas the ICC between the reference standard and the estimation at level L3 were globally lower, notably with $\mathrm{FBM_{Manual\_L3}}$ (0.84), $\mathrm{VAT_{Manual\_L3}}$ (0.65), and $\mathrm{SAT_{Manual\_L3}}$ (0.77). However, the ICC between $\mathrm{MBM_{REF}}$ and $\mathrm{MBM_{Manual\_L3}}$ was good (0.98 with 95% CI of 0.95–0.99). Concerning the Bland–Altman plots, all mean differences between the reference standard and Anthropometer3D were small (< 3.5% points or difference) with narrow 95% CI (maximal range of − 11.8 to +

Table 1 Patient characteristics

	Mean (SD) [range], unless otherwise stated
Age (year)	56.9 (12.8) [23–74]
Weight (kg)	75.7 (15.7) [45–116]
Size (m)	1.67 (0.07) [1.51–1.83]
Body mass index (kg/m^2)	27.1 (4.6) [18.4–39.9]
Sex	Men, 15 (50%)
	Women, 15 (50%)
Diseases	Melanoma (14)
	Inflammatory disease (9)
	Lymphoma (4)
	Myeloma (2)
	Other (1)

Table 2 Mean, standard deviation, and minimal and maximal values for LBM, FBM, MBM, VAT, and SAT measured manually on a whole-body CT, estimated by Anthropometer3D and estimated by using a slice segmented manually at L3

Mean in kg (SD) [min-max]	Reference standard: whole-body manual segmentation	Anthropometer3D	Manual segmentation at level L3
LBM	47.3 (10.6) [31.6–71.9]	47.5 (10.1) [33.8–72.1]	50.6 (11.7) [34.3–82.9]
FBM	28.1 (10.2) [14.1–58.4]	27.9 (10.5) [12.2–55.2]	29.2 (6.9) [17.0–42.4]
MBM	37.8 (10.1) [22.5–63.9]	37.0 (9.8) [21.2–61.9]	43.2 (10.1) [29.0–69.4]
VAT	4.2 (2.1) [1.2–9.1]	4.3 (2.0) [1.4–8.8]	4.4 (2.2) [1.1–10.0]
SAT	23.9 (9.1) [12.5–54.8]	23.5 (9.6) [10.7–53.8]	24.4 (9.5) [10.8–53.3]

FBM fat body mass, *MBM* muscle body mass, *LBM* lean body mass, *SAT* subcutaneous adipose tissue, *VAT* visceral adipose tissue

14.7% for $FBM_{Anthropo3D}$). Compared with Anthropometer3D, the mean difference between the reference standard and the manual segmentation at L3 was larger except for SAT_{Manual_L3} (− 1.5% for SAT_{Manual_L3} vs + 2.5% for $SAT_{Anthropometer3D}$), and the 95%CIs were globally larger for all the parameters (up to − 78 to 69% for VAT_{Manual_L3}).

Dice's coefficients between the reference method and Anthropometer3D for the three types of segmented voxels were excellent with mean ± SD (min-max) of 0.95 ± 0.02 (0.90–0.97) for muscles, 1.00 ± 0.01 (0.97–1.00) for fat, and 0.97 ± 0.02 (0.90–0.99) for visceral adipose tissue.

Discussion

We have developed and validated a new software allowing the automatic measurement in multi-slices of several anthropometric parameters: fat, lean, and muscle body mass, but also subcutaneous and visceral adipose tissue. Anthropometer3D is based on a multi-atlas segmentation method from CT of PET/CT with a large range of acquisition, from the ischium to the eyes. The measurements performed by Anthropometer3D gave very consistent results compared with the reference method, which was a manual segmentation of the CT over the whole

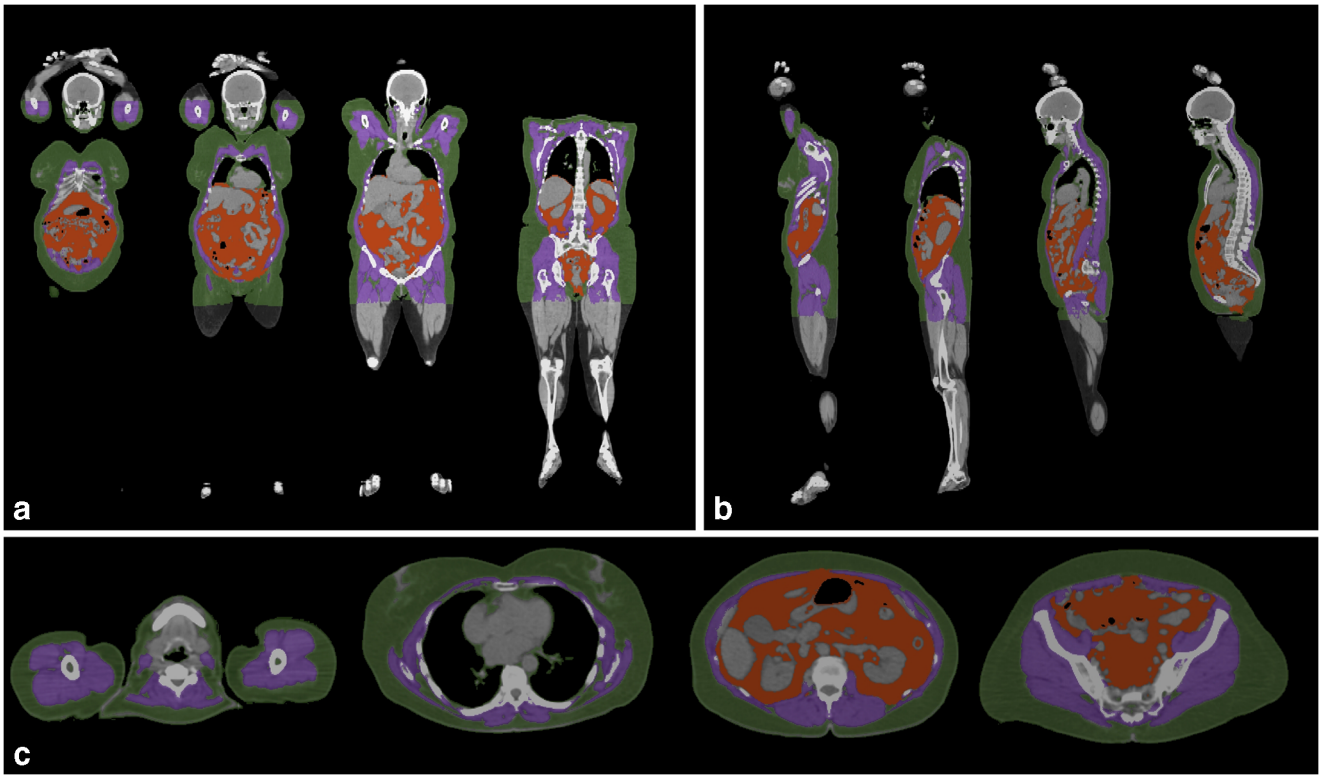

Fig. 2 Visual representation of the multi-slice and automatic segmentation of voxels of fat (green and red), muscle (purple), and visceral adipose tissue (red) from the ischium to the eyes on **a** frontal, **b** sagittal, and **c** axial views of a whole-body CT

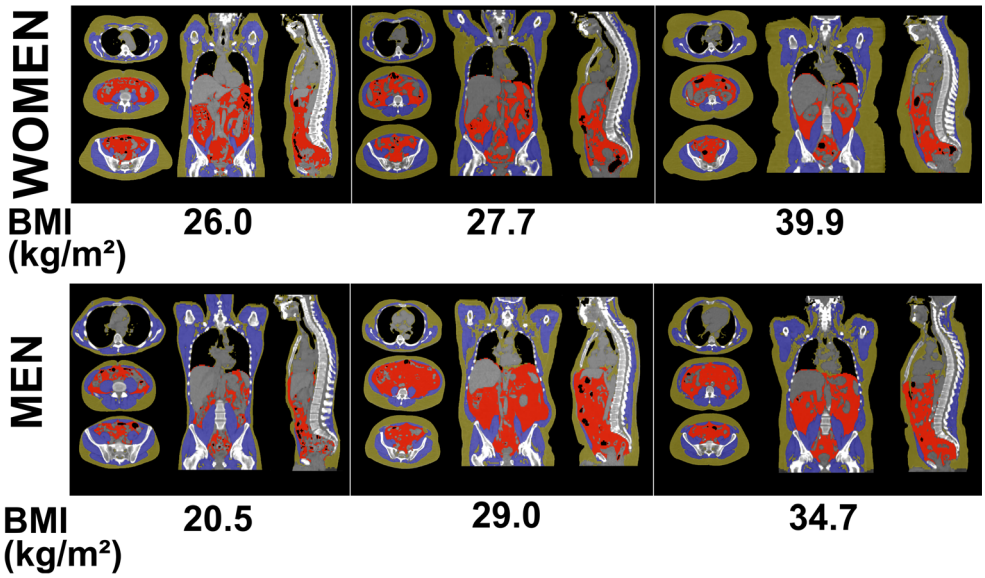

Fig. 3 Visual representation of the multi-slice and automatic segmentation of voxels of subcutaneous fat (yellow), muscle (purple), and visceral fat (red) of six patients (three women and three men) with different body mass index (BMI)

body. The ICC values between the two methods were close to 1, and the Bland–Altman plots showed a small mean difference and a narrow 95%CI for the five parameters measured compared with manual whole-body segmentation. These good results can be explained by the accuracy of the MAS, but also by the use of extrapolation factors (k_{muscle} and k_{fat}), which were relatively stable between the patients.

For patients with cancer, the measurement of anthropometric parameters is becoming increasingly important, particularly to explore prognosis or to adapt treatment [34]. However, body composition generally requires segmentation of medical images. Multi-slice measurement is more accurate than measurement of one slice, but it also takes longer when the segmentation is performed manually [19]. A compromise must, therefore, be found between the duration of the segmentation and the accuracy of the measurement, justifying the development of Anthropometer3D.

Many algorithms already exist to segment anthropometric parameters on CT or MRI. Most of them are based on a 2D segmentation method, notably at level L3 [22, 35], and their accuracy is, therefore, limited due to the use of one slice. Moreover, they cannot theoretically be better than a manual mono-slice segmentation, which was used in this study to evaluate the accuracy of a mono-slice measurement. To perform a 3D segmentation of these parameters, few automatic segmentation methods have been proposed (e.g., region growing, graph cutting, fuzzy C means clustering, and MAS algorithms) [22]. Most of them are based on the determination of the muscle boundary between VAT and SAT [22]. MAS methods have been shown to be very flexible, allowing them to capture anatomical variations, notably between different levels of the body, such as the abdomen and the pelvis [23], whereas other algorithms must be adapted according to the anatomical level [22, 24, 36].

Therefore, MAS algorithms have been used successfully to segment multiple anthropometric parameters on MRI images [37]. Those measurements, however, require a dedicated examination with, for example, a specific dual-echo Dixon Vibe protocol covering the neck to the knees. Rather than using a dedicated examination (MRI or CT), our method was developed and validated on an already existing CT of a PET/CT acquisition, which is frequently available for patients with cancer, avoiding an additional cost in time, personnel, money, and potentially, radiation exposure [16]. Furthermore, the use of a CT allows the creation of a more simplified, and therefore robust, algorithm as the Hounsfield units of the fat and muscle tissue are well standardized and easily isolated by thresholding [13]. In contrast, the isolation of tissues on MRI requires a more complex pre-processing, notably linked to the inhomogeneities of the signal [22].

MAS can also be associated with other segmentation methods to improve segmentation. Xu et al. have, therefore, proposed an augmented active shape model by integrating MAS and level set techniques into the traditional active shape model framework [38]. On 20 CT scans, their segmentation method on the whole abdominal wall allowed subcutaneous and visceral fat measurement. High correlations were observed between their method and the measurement derived from manual segmentation (Pearson's correlation coefficient of 0.94 for the subcutaneous tissue and 0.96 for the visceral tissue) [38] with a good Dice coefficient (0.86 ± 0.09).

With MAS algorithms, the segmentation accuracy depends on the initial database, the registration process, the labeled parts of the atlases, and the selection of the label. The good performances of Anthropometer3D show that our methodological choices were relevant. The use of a rigid registration followed by an elastic registration is a classical registration method [23]. However, we improved this model significantly

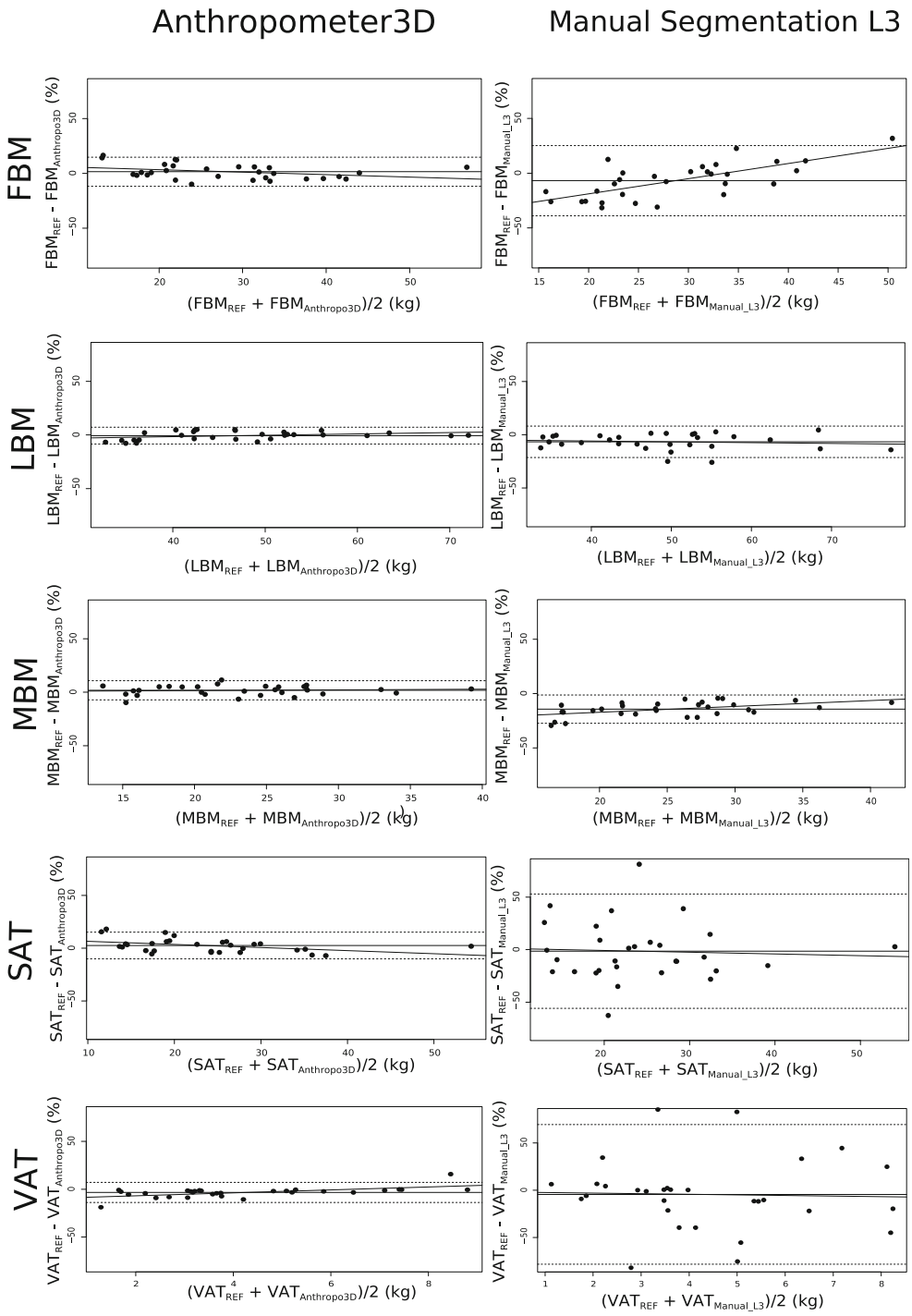

Figure 4 Bland-Altman plots of LBM, FBM, MBM, VAT, and SAT computed using Anthropometer3D and a slice segmented manually at L3 with respect to the whole-body CT segmented manually as the reference standard

by using the rigid registration part to calculate the extrapolation factors of the body parts beyond the eyes and the ischium and to select the ten more similar CTs having subsequent elastic registration, therefore saving processing time. For the elastic registration, we used the registration software Plastimatch, which is freely available and has an implementation of the demons algorithm [39]. The results were good with this tool, but other software and algorithms, such as Elastix with the B-splines algorithm, could be used [17]. As the labeled part of the atlas, we used three different types of mask (body shape, abdominal cavity, and muscles) corresponding more to regions than organs. The combination of multi-atlas segmentation of regions followed by windowing based on HU values of fat and muscle allows a better segmentation, as these parts are anatomically more stable than organs between all patients [17]. As shown by Morsbach et al. [40], it has to be noted that changing the CT's kV can have an impact on HU values. In their study, they found that the mean attenuation

Table 3 ICC and Bland–Altman plot results (mean difference and 95%CI) for FBM, LBM, MBM, VAT, and SAT estimated by Anthropometer3D and a slice segmented manually at L3 with respect to the whole-body CT segmented manually as the reference standard

	Anthropometer3D	Manual segmentation at L3
ICC between the reference standard and the tested method		
LBM	0.99 (0.97–0.99)	0.93 (0.86–0.97)
FBM	0.99 (0.97–0.99)	0.84 (0.68–0.92)
MBM	0.99 (0.97–0.99)	0.98 (0.95–0.99)
VAT	0.99 (0.98–1.00)	0.65 (0.39–0.82)
SAT	0.99 (0.98–1.00)	0.77 (0.57–0.88)
Bland–Altman plot: mean difference (in %) [95%CI]		
LBM	− 0.7 [− 8.5; 7.2]	− 6.7 [− 21.4; 8.1]
FBM	1.5 [− 11.8; 14.7]	− 6.9 [− 38.9; 25.2]
MBM	1.8 [− 7.1; 10.8]	14.3 [− 27.4; − 1.3]
VAT	− 3.3 [− 13.9; 7.2]	− 4.4 [− 78.2; 69.3]
SAT	2.5 [− 10.2; 15.2]	− 1.5 [− 55.9; 52.9]

FBM fat body mass, *MBM* muscle body mass, *LBM* lean body mass, *SAT* subcutaneous adipose tissue, *VAT* visceral adipose tissue

coefficient for muscle was 48± 11 HU at 80 kV vs 41 ± 9 HU at 140 kV ($p < 0.01$). Fat mean attenuation coefficient was − 84± 10 HU at 80 kV vs − 69± 6 HU at 140 kV ($p < 0.01$). However, the impact of these differences on the surfaces measured at level L3 were quite limited, notably for the adipose tissue: the mean total muscle area was 117 ± 35 cm^2 at 80 kV vs 123 ± 35 cm^2 at 140 kV ($p<0.01$) and the adipose tissue index was 54.5 ± 31.3 cm^2/m^2 at 80 kV vs 54.2 ± 32.6 cm^2/m^2 at 140 kV ($p = 0.39$). Yamada et al. [41] found also that visceral adipose surface was not statistically different between standard-dose and low-dose CT. In a study evaluating the muscles at the L3 level, Fuchs et al. found that low tube current significantly decreased the mean total muscle by 4.79% (6.44 cm^2; minimum 3.78, maximum 9.10) [42]. However, the impact of the tissue thresholds according to the change of kV has yet to be evaluated for multi-slice segmentations, an adaptation of the threshold according to kV being possibly useful. For the selection of voxel label, we used majority voting, which is common. Other methods, such as the SIMPLE algorithm, could be used, but the potential improvement could be minor at the detriment of computation time [17]. We chose a pixel size of 1.36 × 1.36 × 5 mm^3 as a compromise to get a good anatomical resolution with fast processing time. Other pixel sizes are possible, smaller pixels being, however, prone to increase the calculation time and larger pixels may be subject to a decrease in anatomical resolution.

Our population was morphologically very heterogeneous with different BMIs, ages, and gender. This heterogeneity is an advantage for the MAS method as it helps to capture morphological variability. We have chosen to take normal examinations to create the Anthopometer3D atlas, as this offers better adaptability for the segmentation of new CT data (normal or with tumors).

Moreover, the Dice coefficient was maximal for fat voxels with a mean value of 1.0. This value can be explained by the rather similar fat voxel isolation method between the reference standard [16] and Anthropometer3D which are notably based on a Hounsfield threshold between − 190 and – 30 HU to isolate fat tissues. Compared to the reference standard, Anthropomer3D is however fully automatic and associated with the segmentation of other tissues like muscle and visceral adipose tissue.

Finally, if the MAS method can be quite time consuming (approximately 25 min for each patient in our study with a CPU of 2.5 GHz), this difference has to be tempered, as the speed of calculation improves year after year, notably when using graphics processing unit (GPU) implementation. Moreover, this automatic processing time remains is not comparable with the manual segmentation of a whole-body CT which, in this study, it took more than 6 h for each patient. To improve the processing time, we are considering the use of a 3D neural network segmentation method based on a GPU implementation. However, this type of segmentation needs, for the training, a far higher number of whole-body CT manually segmented than MAS method which gave good results in our study with only 30 patients manually segmented. To compare, Lee et al. [35] used a neural network for the automatic segmentation of a 2D unique abdominal slice with 250 manually segmented image slices needed for the training and a comparable number of time consuming manually segmented whole-body CT can be expected for a 3D whole-body segmentation.

Conclusion

Anthropometer3D allows automatic measurement of multiple anthropometric parameters based on a multi-slice segmentation. It is more precise than estimates generally made using segmentation at the L3 level. This tool could be applied automatically on large clinical databases, notably to explore new prognostic factors.

References

1. Prado CMM, Lieffers JR, McCargar LJ, Reiman T, Sawyer MB, Martin L et al.: Prevalence and clinical implications of sarcopenic obesity in patients with solid tumours of the respiratory and gastrointestinal tracts: A population-based study. Lancet Oncol 9:629–635, 2008

2. Bye A, Sjøblom B, Wentzel-Larsen T, Grønberg BH, Baracos VE, Hjermstad MJ, Aass N, Bremnes RM, Fløtten Ø, Jordhøy M: Muscle mass and association to quality of life in non-small cell lung cancer patients. J Cachexia Sarcopenia Muscle 8:759–767, 2017
3. Lieffers JR, Bathe OF, Fassbender K, Winget M, Baracos VE: Sarcopenia is associated with postoperative infection and delayed recovery from colorectal cancer resection surgery. Br J Cancer 107: 931–936, 2012
4. Blauwhoff-Buskermolen S, Versteeg KS: de van der Schueren MAE, den braver NR, Berkhof J, Langius JAE, et al. loss of muscle mass during chemotherapy is predictive for poor survival of patients with metastatic colorectal Cancer. J Clin Oncol 34:1339–1344, 2016
5. Shen W, Wang Z, Punyanita M, Lei J, Sinav A, Kral JG, Imielinska C, Ross R, Heymsfield SB: Adipose tissue quantification by imaging methods: A proposed classification. Obes Res 11:5–16, 2003
6. Lauby-Secretan B, Scoccianti C, Loomis D, Grosse Y, Bianchini F, Straif K: Body fatness and Cancer — Viewpoint of the IARC working group. N Engl J Med 375:794–798, 2016
7. Gouérant S, Leheurteur M, Chaker M, Modzelewski R, Rigal O, Veyret C et al.: A higher body mass index and fat mass are factors predictive of docetaxel dose intensity. Anticancer Res 33:5655–5662, 2013
8. Camus V, Lanic H, Kraut J, Modzelewski R, Clatot F, Picquenot JM, Contentin N, Lenain P, Groza L, Lemasle E, Fronville C, Cardinael N, Fontoura ML, Chamseddine A, Brehar O, Stamatoullas A, Leprêtre S, Tilly H, Jardin F: Prognostic impact of fat tissue loss and cachexia assessed by computed tomography scan in elderly patients with diffuse large B-cell lymphoma treated with immunochemotherapy. Eur J Haematol 93:9–18, 2014
9. Iwase T, Sangai T, Nagashima T, Sakakibara M, Sakakibara J, Hayama S, Ishigami E, Masuda T, Miyazaki M: Impact of body fat distribution on neoadjuvant chemotherapy outcomes in advanced breast cancer patients. Cancer Med 5:41–48, 2016
10. Gu W, Zhu Y, Wang H, Zhang H, Shi G, Liu X, Ye D: Prognostic value of components of body composition in patients treated with targeted therapy for advanced renal cell carcinoma: A retrospective case series. PLoS One 10:e0118022, 2015
11. Slaughter KN, Thai T, Penaroza S, Benbrook DM, Thavathiru E, Ding K, Nelson T, McMeekin DS, Moore KN: Measurements of adiposity as clinical biomarkers for first-line bevacizumab-based chemotherapy in epithelial ovarian cancer. Gynecol Oncol 133: 11–15, 2014
12. Buckinx F, Landi F, Cesari M, Fielding RA, Visser M, Engelke K, Maggi S, Dennison E, al-Daghri NM, Allepaerts S, Bauer J, Bautmans I, Brandi ML, Bruyère O, Cederholm T, Cerreta F, Cherubini A, Cooper C, Cruz-Jentoft A, McCloskey E, Dawson-Hughes B, Kaufman JM, Laslop A, Petermans J, Reginster JY, Rizzoli R, Robinson S, Rolland Y, Rueda R, Vellas B, Kanis JA: Pitfalls in the measurement of muscle mass: A need for a reference standard. J Cachexia Sarcopenia Muscle 9:269–278, 2018
13. Chowdhury B, Sjöström L, Alpsten M, Kostanty J, Kvist H: Löfgren R. A multicompartment body composition technique based on computerized tomography. Int J Obes Relat Metab Disord 18:219–234, 1994
14. Malnick SDH, Melzer E: It is not ethical to perform a CT scan purely for determining visceral fat. J Clin Gastroenterol 50:352, 2016
15. Mourtzakis M, Prado CMM, Lieffers JR, Reiman T, McCargar LJ, Baracos VE: A practical and precise approach to quantification of body composition in cancer patients using computed tomography images acquired during routine care. Appl Physiol Nutr Metab 33: 997–1006, 2008
16. Decazes P, Métivier D, Rouquette A, Talbot JN, Kerrou K: Method to improve the semiquantification of 18F-FDG uptake: Reliability of the estimated lean body mass using the conventional, low-dose CT from PET/CT. J Nucl Med 57:753–758, 2016
17. Decazes P, Rouquette A, Chetrit A, Vera P, Gardin I: Automatic measurement of the total visceral adipose tissue from computed tomography images by using a multi-atlas segmentation method. J Comput Assist Tomogr 42:139-145, 2018
18. Schweitzer L, Geisler C, Pourhassan M, Braun W, Glüer C-C, Bosy-Westphal A, Müller MJ: What is the best reference site for a single MRI slice to assess whole-body skeletal muscle and adipose tissue volumes in healthy adults? Am J Clin Nutr 102:58–65, 2015
19. Shen W, Chen J, Gantz M, Velasquez G, Punyanitya M, Heymsfield SB: A single mri slice does not accurately predict visceral and subcutaneous adipose tissue changes during weight loss. Obesity 20:2458–2463, 2012
20. Thomas EL, Bell JD: Influence of undersampling on magnetic resonance imaging measurements of intra-abdominal adipose tissue. Int J Obes Relat Metab Disord 27:211–218, 2003
21. Schaudinn A, Linder N, Garnov N, Kerlikowsky F, Blüher M, Dietrich A, Schütz T, Karlas T, Kahn T, Busse H: Predictive accuracy of single- and multi-slice MRI for the estimation of total visceral adipose tissue in overweight to severely obese patients. NMR Biomed 28:583–590, 2015
22. Hu HH, Chen J, Shen W: Segmentation and quantification of adipose tissue by magnetic resonance imaging. MAGMA 29:259–276, 2016
23. Iglesias JE, Sabuncu MR: Multi-atlas segmentation of biomedical images: A survey. Med Image Anal 24:205–219, 2015
24. Kullberg J, Johansson L, Ahlström H, Courivaud F, Koken P, Eggers H, Börnert P: Automated assessment of whole-body adipose tissue depots from continuously moving bed MRI: A feasibility study. J Magn Reson Imaging 30:185–193, 2009
25. Karlsson A, Rosander J, Romu T, Tallberg J, Grönqvist A, Borga M, Dahlqvist Leinhard O: Automatic and quantitative assessment of regional muscle volume by multi-atlas segmentation using whole-body water-fat MRI. J Magn Reson Imaging 41:1558–1569, 2015
26. Anthropometer 3D | Automatic 3D anthropometry from medical images [Internet]. [accessed 2018 May 28]. Available from: https://www.anthropometer3d.org/
27. Taha AA, Hanbury A: Metrics for evaluating 3D medical image segmentation: Analysis, selection, and tool. BMC Med Imaging 15: 29, 2015
28. J Mendez, Keys A. Density and composition of mammalian muscle. Metabolism. 9:184-188, 1960
29. Seg3D [Internet]. [accessed 2018 Feb 5]. Available from: http://www.sci.utah.edu/cibc-software/seg3d.html
30. Lee J, Koh D, Ong CN: Statistical evaluation of agreement between two methods for measuring a quantitative variable. Comput Biol Med 19:61–70, 1989
31. Bland JM, Altman DG: Statistical methods for assessing agreement between two methods of clinical measurement. Lancet 1:307–310, 1986
32. Dice LR: Measures of the amount of ecologic association between species. Ecology 26:297–302, 1945
33. Team RDC: R: A language and environment for statistical computing [Internet] [accessed 2018 May 28]. Vienna: R Foundation for Statistical Computing, 2008, Available from: http://www.R-project.org
34. Jacquelin-Ravel N, Pichard C: Clinical nutrition, body composition and oncology: A critical literature review of the synergies. Crit Rev Oncol Hematol 84:37–46, 2012
35. Lee H, Troschel FM, Tajmir S, Fuchs G, Mario J, Fintelmann FJ, Do S: Pixel-level deep segmentation: Artificial intelligence quantifies muscle on computed tomography for body morphometric analysis. J Digit Imaging 30:487–498, 2017
36. Kullberg J, Hedström A, Brandberg J, Strand R, Johansson L, Bergström G, Ahlström H: Automated analysis of liver fat, muscle and adipose tissue distribution from CT suitable for large-scale studies. Sci Rep 7:10425, 2017

37. Middleton MS, Haufe W, Hooker J, Borga M, Dahlqvist Leinhard O, Romu T, Tunón P, Hamilton G, Wolfson T, Gamst A, Loomba R, Sirlin CB: Quantifying abdominal adipose tissue and thigh muscle volume and hepatic proton density fat fraction: Repeatability and accuracy of an MR imaging-based, Semiautomated analysis method. Radiology 283:438–449, 2017
38. Xu Z, Conrad BN, Baucom RB, Smith SA, Poulose BK, Landman BA: Abdomen and spinal cord segmentation with augmented active shape models. J Med Imaging (Bellingham) 3:036002, 2016
39. Sharp GC, Peroni M, Li R, Shackleford J, Kandasamy N: Evaluation of plastimatch B-spline registration on the EMPIRE10 data set. Medical Image Analysisfor the Clinic: A Grand Challenge 99–108, 2010
40. Morsbach F, Zhang Y-H, Nowik P, Martin L, Lindqvist C, Svensson A, Brismar TB: Influence of tube potential on CT body composition analysis. Nutrition 53:9–13, 2018
41. Yamada Y, Jinzaki M, Niijima Y, Hashimoto M, Yamada M, Abe T, Kuribayashi S: CT dose reduction for visceral adipose tissue measurement: Effects of model-based and adaptive statistical iterative reconstructions and filtered Back projection. AJR Am J Roentgenol 204:W677–W683, 2015
42. Fuchs G, Chretien YR, Mario J, Do S, Eikermann M, Liu B, Yang K, Fintelmann FJ: Quantifying the effect of slice thickness, intravenous contrast and tube current on muscle segmentation: Implications for body composition analysis. Eur Radiol 28:2455–2463, 2018